Supramolecular binding of protonated amines to a receptor microgel in aqueous buffer

Alan Tominey, David Andrew, Georgina M. Rosair, Lewis Oliphant, Juliette Dupré and Arno Kraft*

Chemistry, School of Engineering & Physical Sciences, Heriot-Watt University, Riccarton, Edinburgh EH14 4AS, United Kingdom

Supporting Information

General. All the chemicals used were reagent grade and used without further purification. ^{1}H NMR (400 MHz) experimental spectra were obtained with a Bruker DPX400 spectrometer. Ultrafiltration was carried out using a Masterflex 7518-00 peristaltic pump with a Vivaflow 50 PES polysulfone filter (MWCO 100,000).

Microgel synthesis

In a typical microgel synthesis, a solution of NIPAM **1** (1.13 g, 10 mmol), **2** (0.15 g, 1 mmol), **3-Na** (0.14 g, 0.8 mmol), and sodium dodecylsulfate (60 mg, 0.2 mmol) in water (200 mL) was heated to 70 °C and degassed with N_2 for 15 minutes. Ammonium persulfate (60 mg, 0.5 mmol) was added, and the reaction was stirred overnight at 70 °C. The reaction mixture became turbid soon after the start of the polymerisation. Ultrafiltration (Vivaflow 50 polysulfone membrane, cut-off 100,000 g/mol) against 2 L of deionised water, followed by concentration under a vacuum and freeze-drying, gave the purified microgel as a colourless solid. Yield: 1.10 g.

Determination of reactivity ratios for copolymerisation of NIPAM and monomer 3-Na

Reactivity ratios of the two monomers NIPAM and MAA involved in a reaction of copolymerisation were determined by a method recently described in the literature.[1,2] This method consists of following the continuous change of the monomer feed ratio as a function of the time of intensity of the monomers' ^{1}H NMR signals at constant temperature and in the presence of a radical initiator.

A 5-mm-diameter NMR tube was filled with a solution of NIPAM, **3-Na** and initiator $(NH_4)_2S_2O_8$ in 0.7 mL of D_2O. The initial feed concentrations of the monomers were 0.149 mol L^{-1} NIPAM/ 0.188 mol L^{-1} **3-Na** and 0.24 mol L^{-1}/0.088 mol L^{-1}. The concentration of the initiator was comparatively high (ca. 0.08M) to ensure that the polymerisation proceeded within 1 h at 60 °C. Added N,N-(dimethylamino)pyridine (DMAP) served as an internal intensity reference.

A series of ^{1}H NMR spectra were measured on a Bruker DPX400 according to a procedure suggested by Aguilar et al.[1] The temperature was set to 57 °C. Shimming gradients were optimised at this temperature with a neat D_2O sample before the experiment. The free induction decay was recorded every 60 seconds by a 90° pulse and a single scan, and was stored on a hard disk. The NMR spectra thus obtained were processed by Fourier transformation and were phase-corrected.

[1] Aguilar, M. R.; Gallardo, A.; del Mar Fernández, M.; San Román, J. *Macromolecules* **2002**, 35, 2036.

[2] Taden, A.; Tait, A. H.; Kraft, A.; *J. Polymer Sci.*, *Polym. Chem.* **2002**, *40*, 4333.
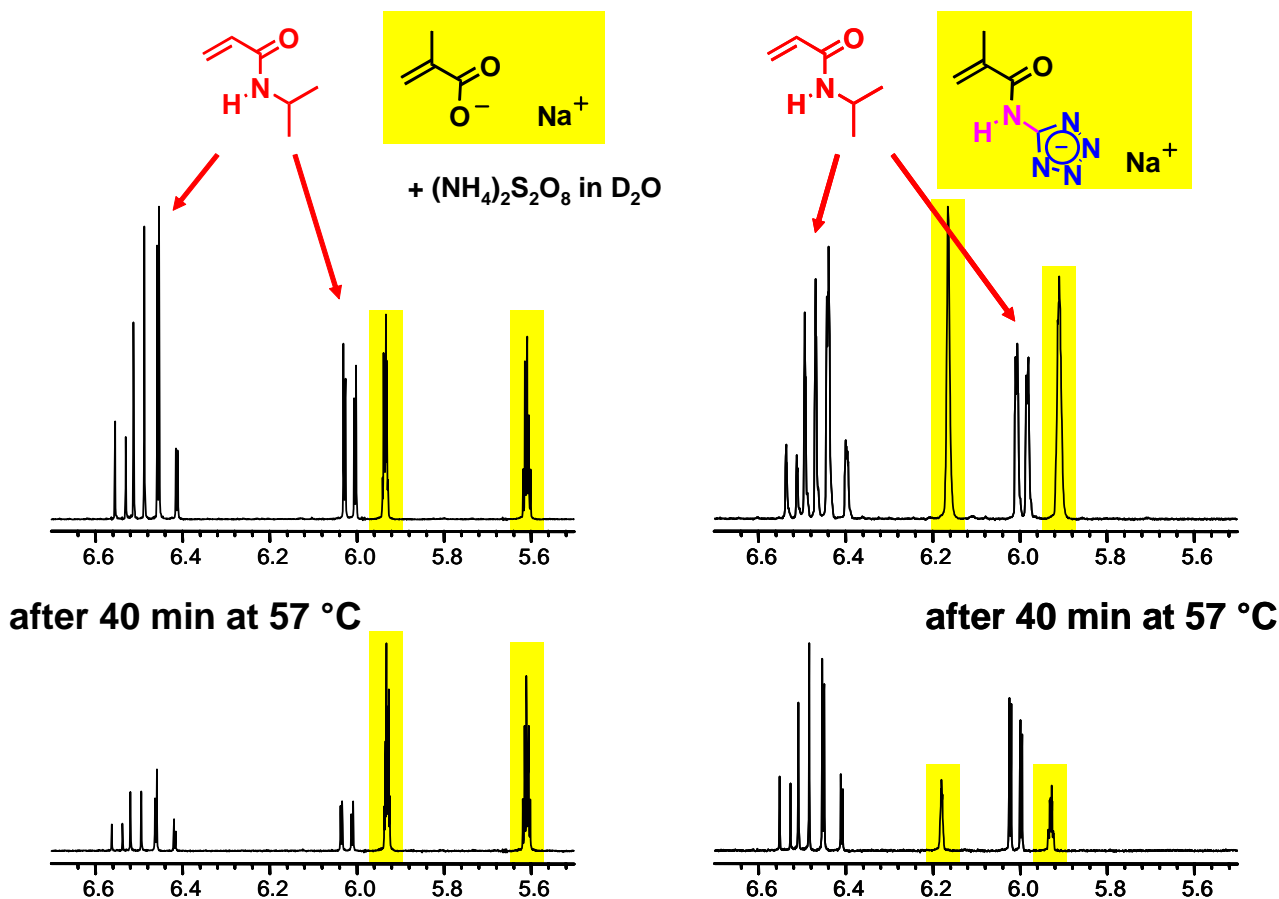
Figure S1. Left: ^{1}H NMR spectra recorded during the copolymerisation of NIPAM and methacrylic acid (NIPAM signals are labelled with arrows, while methacrylic acid signals are highlighted). Starting with an almost equimolar mixture of the two monomers, most of the NIPAM has reacted within 40 min, while the acidic monomer has hardly been consumed. Right: ^{1}H NMR spectra recorded during the copolymerisation of NIPAM and **3-Na** (NIPAM signals are labelled with arrows, while **3-Na** signals are highlighted). In this case, **3-Na** is the more reactive comonomer

Olefinic NMR signals were integrated and normalised to the integration value of the DMAP signals (AA'XX' signal around 8.40 and 7.50 ppm). Normalisation to the inital compositions gave the molar concentrations of the monomers. The as-calculated concentration of **3-Na** was then plotted as a function of

$$x = [NIPAM] / [\textbf{3-Na}]$$

where x is defined as the ratio of the two monomer concentrations, M_1 refers to NIPAM and M_2 to **3-Na**, r_i is the reactivity ratio of the monomer i. The integrated form of the copolymerisation equation can be written as

3

$$[M_2] = k \cdot x^{r_2/(1-r_2)} \cdot [1 - r_2 + (r_1 - 1) \cdot x]^{(r_1 \cdot r_2 - 1)/[(1-r_1)\cdot(1-r_2)]} \qquad \text{eq. 1}$$

in which k is a constant that includes the initial concentrations and takes deviations from the original feed ratio, as might occur during the first couple of minutes of the experiment, into account. The experimental data for [**3-Na**] was fitted to eq. 1 with the use of a "sum-of-squares space" (SS space) approach. To construct the SS space, we varied r_1 and r_2 from 0.01 to 3.00 (excluding 1.00) in increments of 0.01 in Excel 7.0 using a looping structure written in an Excel Visual Basic for Applications module.[1,3]
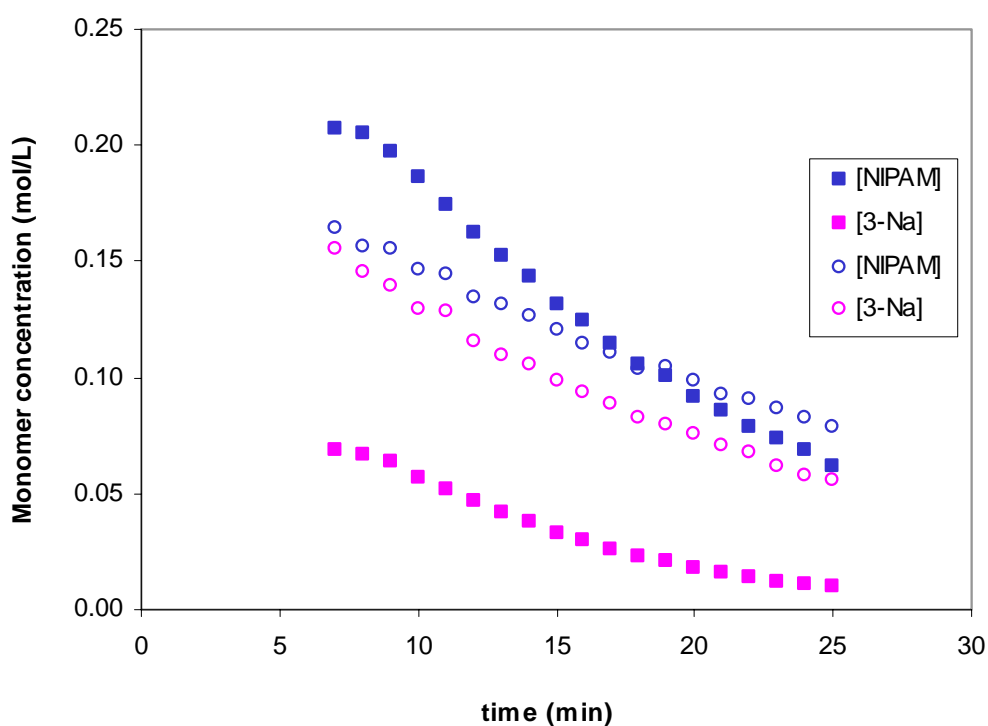

Figure S2. Consumption of the monomers during the copolymerisation of NIPAM and **3-Na**.

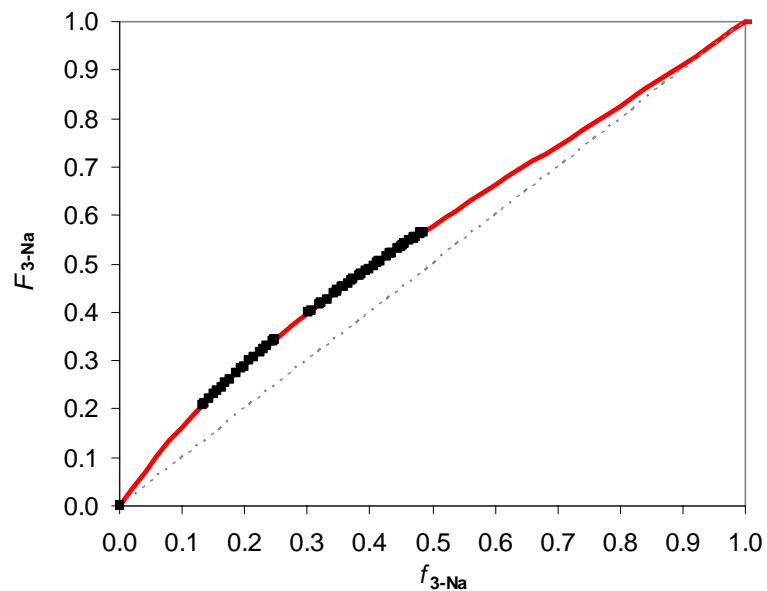[3] Arehart, S. V.; Matyjaszewski, K. *Macromolecules*, **1999**, *32*, 7,2221.

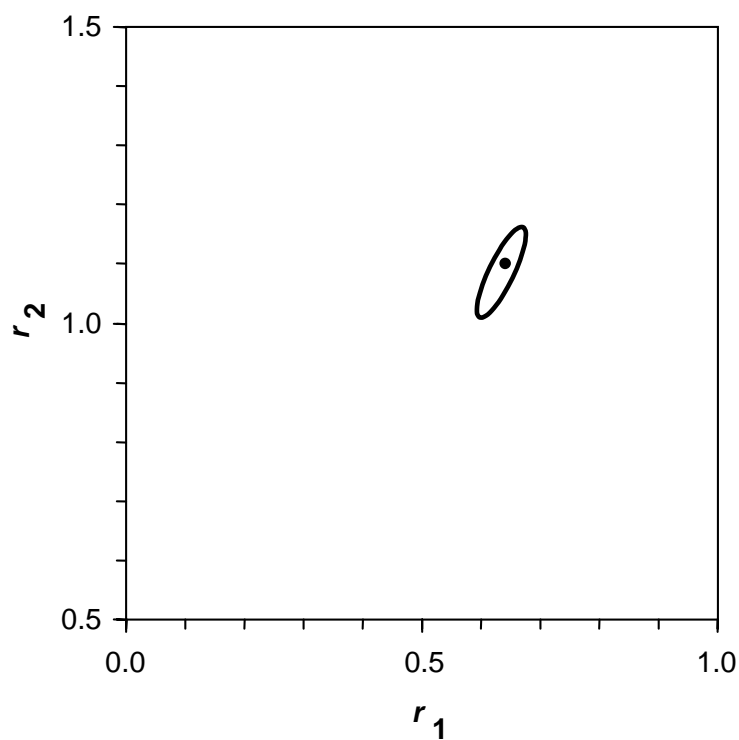**Figure S3.** Calculated copolymer composition diagram showing near-ideal copolymerisation behaviour.

Figure S4. Reactivity ratios with 95% joint confidence limit[4] for the copolymerisation of NIPAM (monomer 1) and tetrazole monomer **3-Na** (monomer 2).

---

[4] A. M. van Herk, *J. Chem. Educ.*, 1995, **72**, 138.

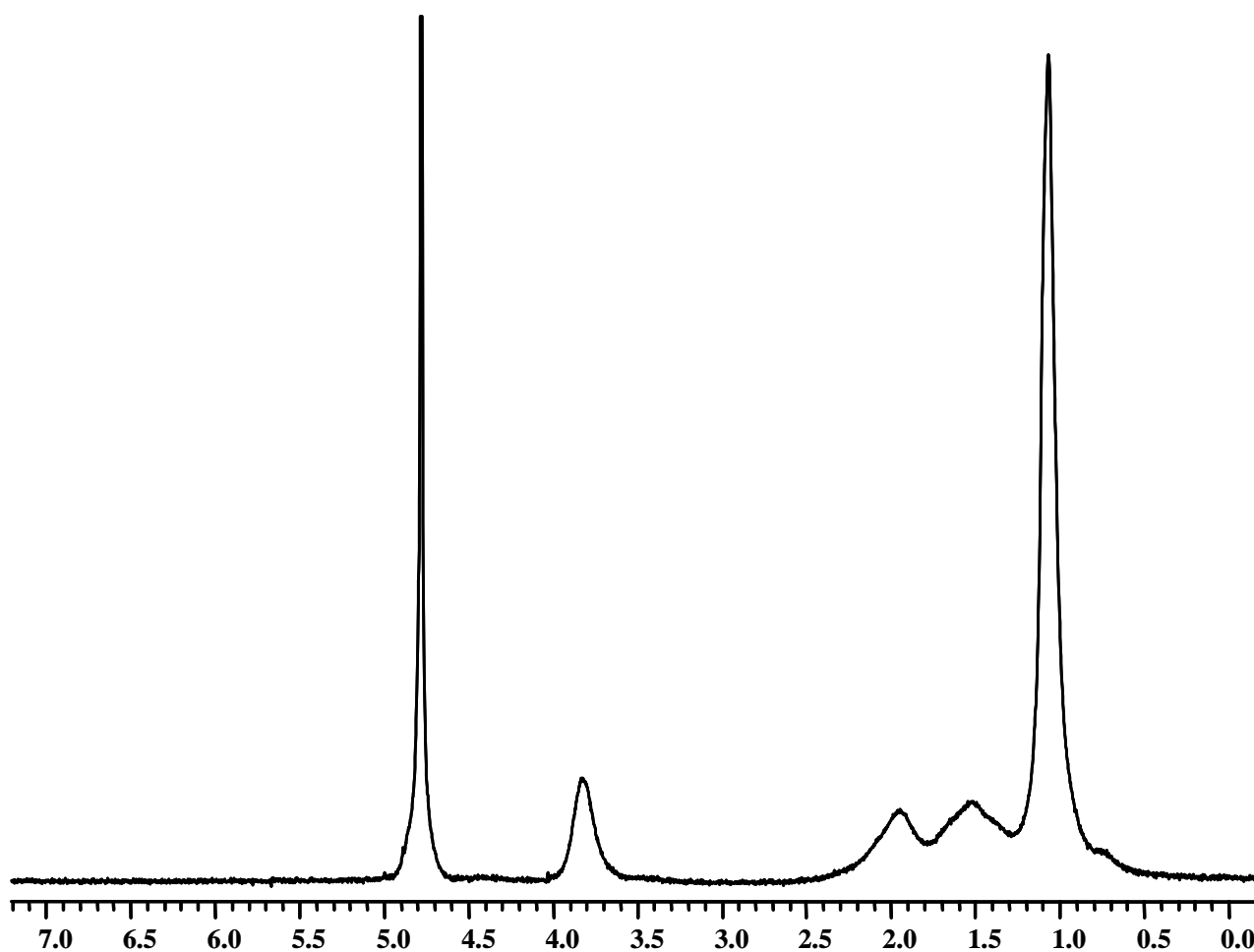**¹H NMR spectrum of the microgel**

Figure S5. 400 MHz ^{1}H NMR spectrum of microgel in D_2O showing the typical broadened signals of a polymer. The ^{1}H NMR spectrum is similar to that of poly-NIPAM, since NIPAM is the major component of the microgel: δ_H 1.06 [broad s, NHCH(CH_3)$_2$], 1.49 and 1.93 (CH and CH$_2$ of polymer backbone), 3.91 (broad s, CH-NH).
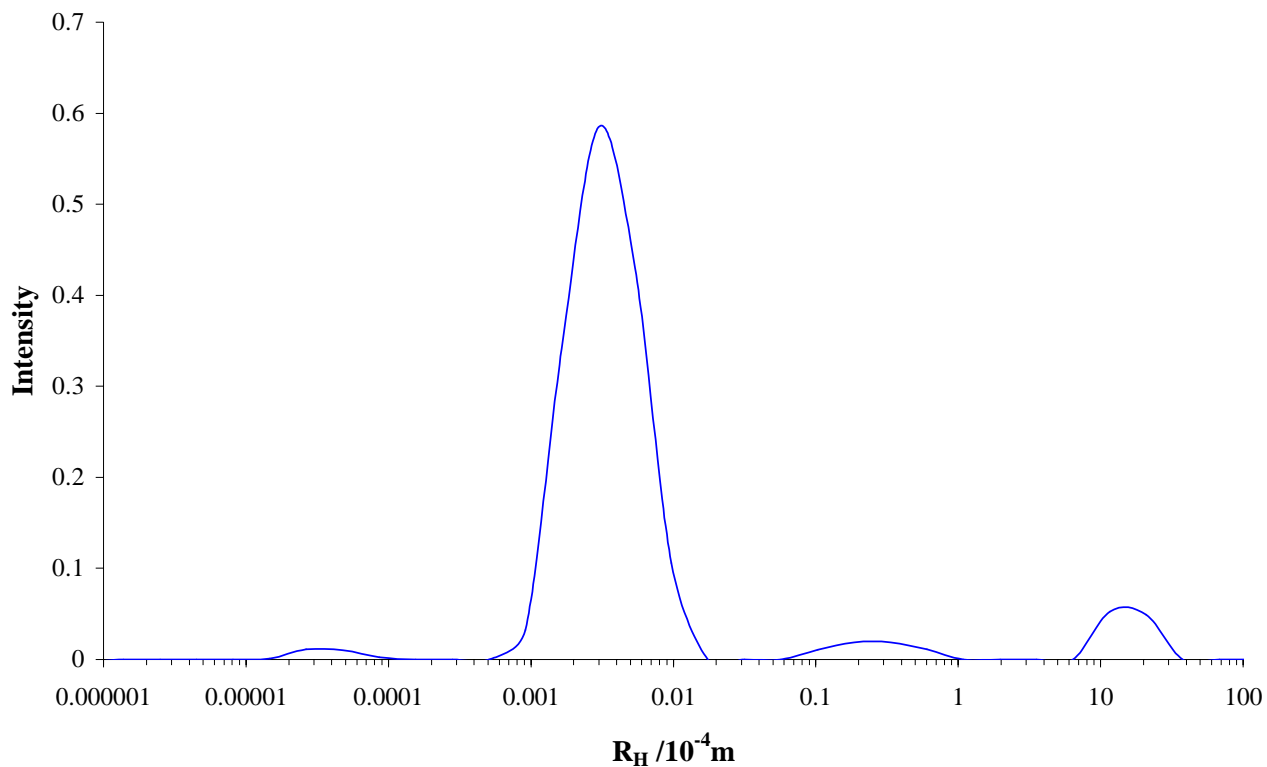
Light scattering measurements

Figure S6. Light scattering results of a dilute aqueous solution of a microgel at 25 °C. The peak of the microgel's size distribution centres around 0.28 µm. Also visible are peaks at higher radii (300 µm and 2 mm) which are attributed to aggregates and (non-crosslinked) polyelectrolyte impurities, although due to their relative intensities they do not comprise a significant concentration within the sample. The small peak at 4.8×10^{-9} m is probably an artifact.
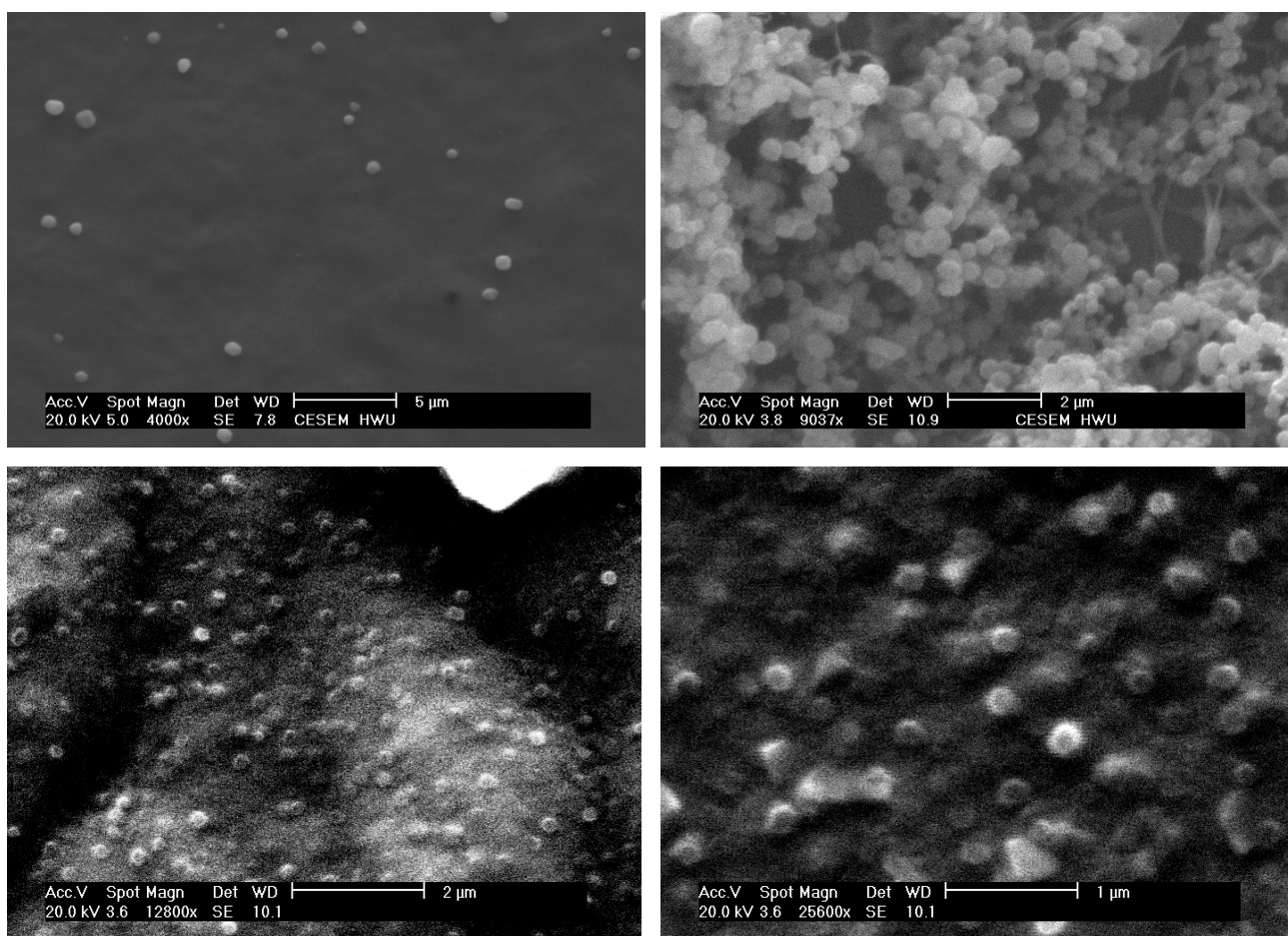
SEM images of microgels

Figure S7. SEM images were taken to further analyse the shape and size of the microgels. Clear images of sufficient quality[5] were obtained after coating a glass substrate with a microgel solution, which was left to dry, followed by covering the substrate with a thin layer of gold. The images show, over different magnification scales, that there is uniformity in the microgel particle size and that the particles are predominantly spherical in shape.

---

[5] E. Nerys, W. Thomas, T. Coakley and C. Winters, *Colloids Surf. B.*, 1996, **6**, 139.
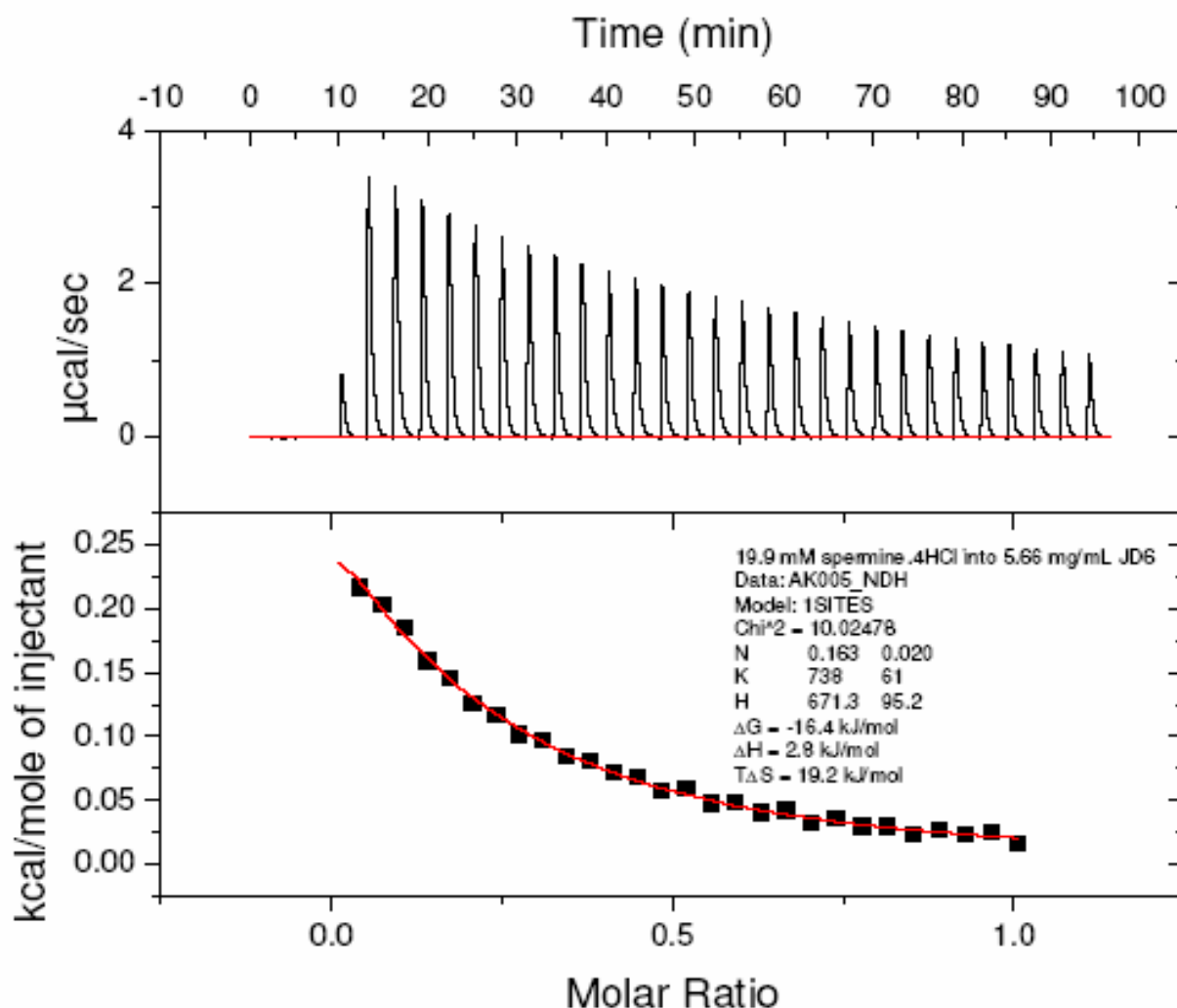
Microcalorimetric data

Figure S8. Microcalorimetry measurements were carried out by dissolving a known quantity of microgel (15–20 mg) in 2.5 mL of a 100 mM morpholine *N*-propanesulfonate (MOPS) pH 7.15 buffer. A spermine hydrochloride solution (dissolved in the same buffer) was then titrated into the microgel solution. The data shown in the figure above was obtained for a microgel containing 10.6 mol% (in the feed) of monomer **3-Na**. The experimental points were fitted to an *n* : 1 binding model and gave the following results: $\Delta G = -16.4$ kJ mol^{-1}, $\Delta H = 2.8$ kJ mol^{-1}, $T\Delta S = 19.2$ kJ mol^{-1}, $K_\text{a} = 738 \pm 61$ M^{-1}.
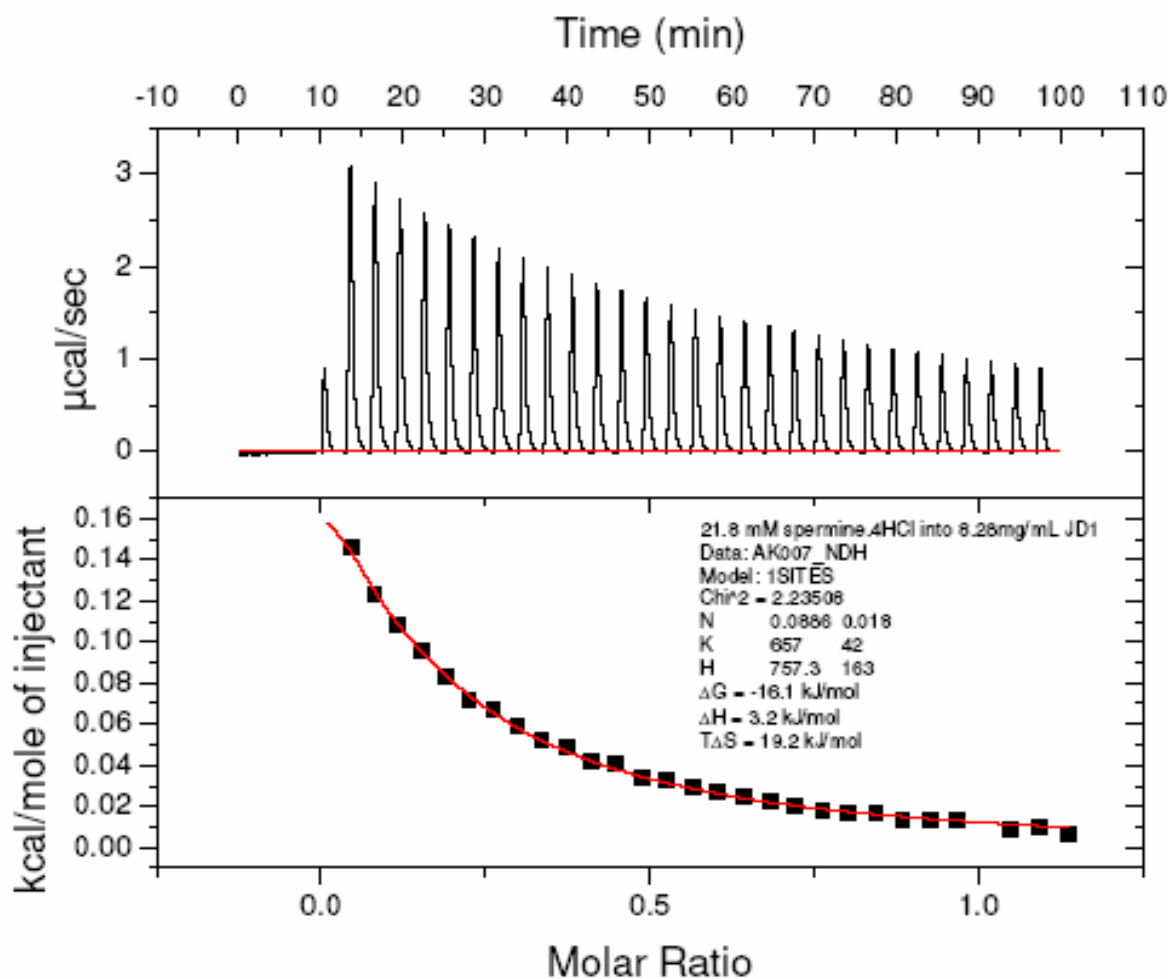
Figure S9. The data shown in the above figure was obtained for a microgel containing 6.8 mol% (in the feed) of monomer **3-Na**. The experimental points were fitted to an $n : 1$ binding model and gave the following results: $\Delta G = -16.1$ kJ mol^{-1}, $\Delta H = 3.2$ kJ mol^{-1}, $T\Delta S = 19.2$ kJ mol^{-1}, $K_a = 657 \pm 42$ M^{-1}.

All D_2O solutions contained a mixture of Na_2HPO_4 and NaH_2PO_4 that served as a pD 7.4 buffer and provided a constant ionic strength during the NMR titration and competition experiments. It also ensured that changes in chemical shift did not occur as a result of proton transfer.

pD Buffer preparation

A pD 7.4 buffer (pD = pH + 0.4) with an ionic strength of 0.15 M was prepared by dissolving 12.0 mg of NaH_2PO_4, 7.0 mg of Na_2HPO_4 and 98 mg of KCl in 10 mL of D_2O at 20 °C. The pD was checked with a calibrated glass electrode.

NMR Binding studies of microgels

Microgel (~ 3 mg) was dissolved in 0.7 mL of D_2O containing a phosphate pD buffer with a constant ionic strength (0.15 M). A stock solution of ligand was also prepared in D_2O at a concentration of 0.454 M in a phosphate pD 7.4 buffer of ionic strength 0.15 M. The stock solution of ligand was titrated into the microgel solution with a digital microliter syringe, and ^{1}H NMR spectra were recorded after each addition.

The stack plots on the following pages were compiled from selected ^{1}H NMR spectra of titrations with various cationic ligands.
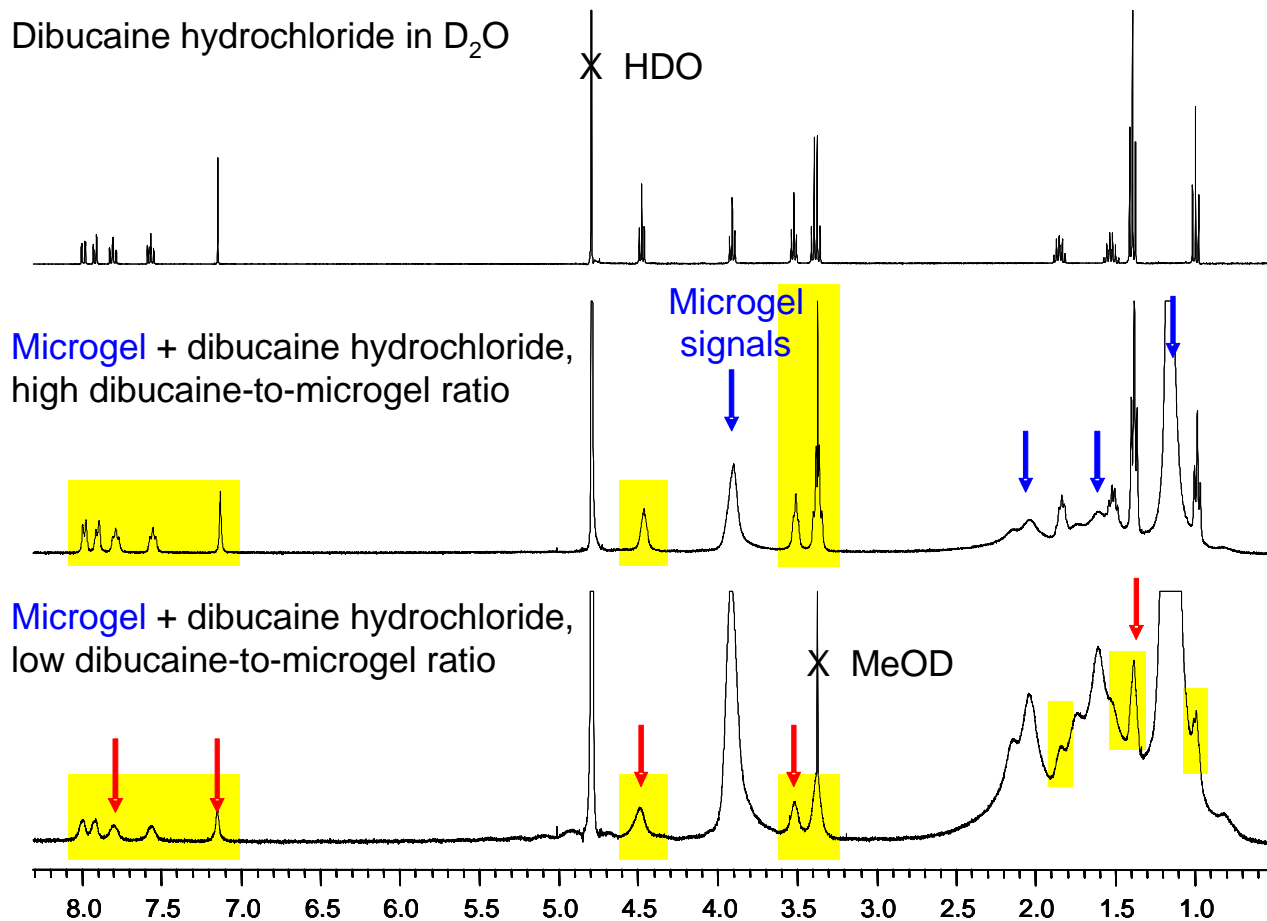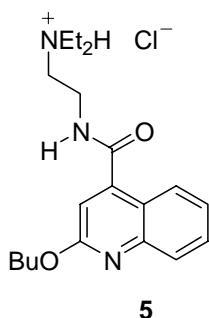
Dibucaine + microgel

5

Figure S10. A ^{1}H NMR spectrum of dibucaine hydrochloride in D_2O buffer (top) shows the typical sharp NMR signals of a low-molecular-weight compound. Line broadening is clearly seen at high microgel-to-dibucaine ratios (bottom). This is indicative of the low-molecular-weight ligand taking up the same tumbling rate as the polymeric microgel when bound. However, the signals of dibucaine sharpen again with increasing amounts of free ligand present as the weighted average shifts towards the unbound fraction and the spectrum clears up (middle). The aromatic signals of the dibucaine ligand lose their resolution, and it is no longer possible to observe any splitting patterns. Addition of more dibucaine led to an increase in the relevant signal heights compared to the microgel signals, while the splitting patterns again began to resolve so that triplets and doublets could again be identified.

Spermidine + microgel
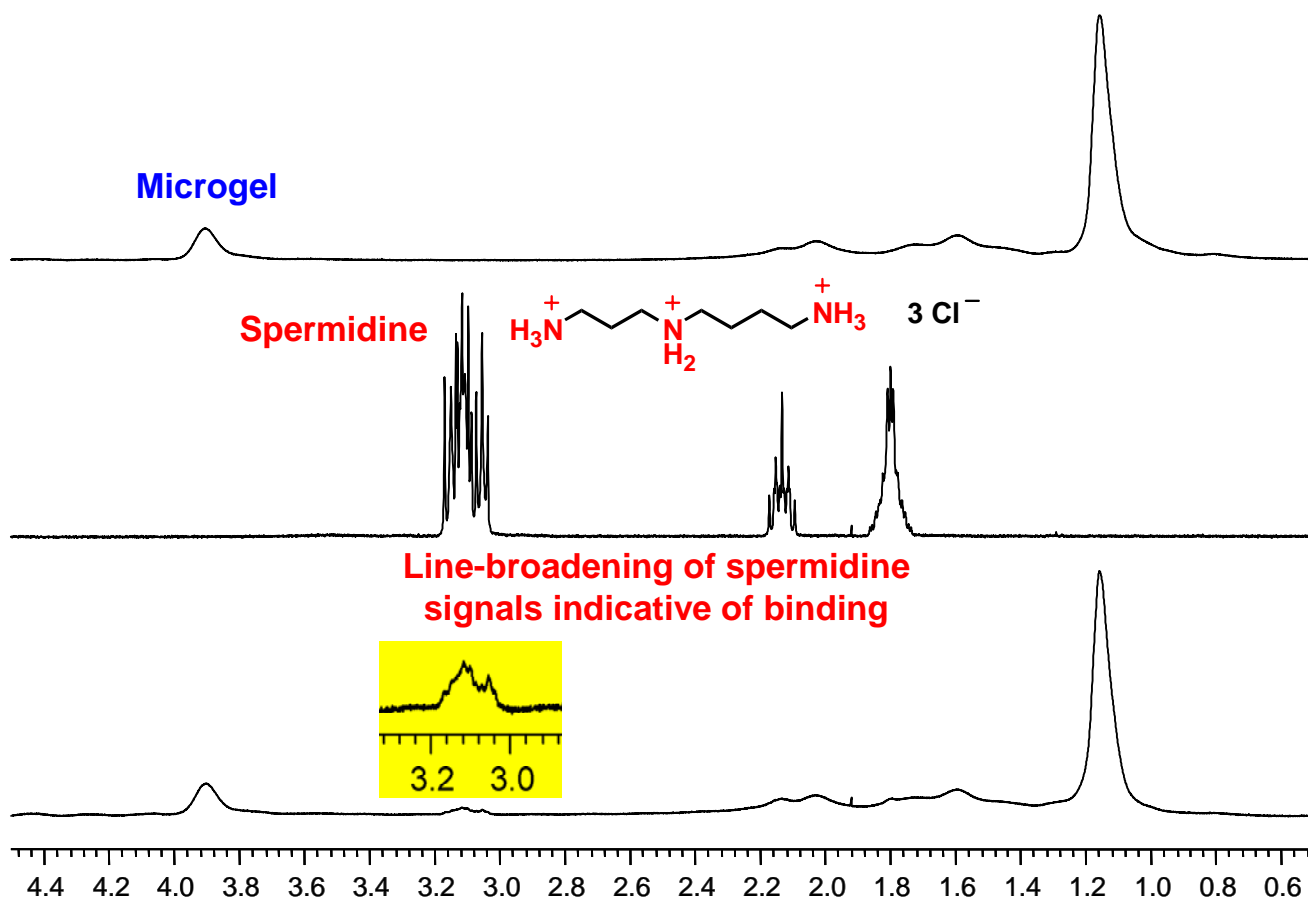
Figure S11. A similar line-broadening effect can also be seen for spermidine in the presence of microgel (bottom NMR spectrum). Microgel concentration: 2.5 mg/0.2 mL. Spermidine trihydrochloride concentration: 2.2 mM.

Propranolol + microgel
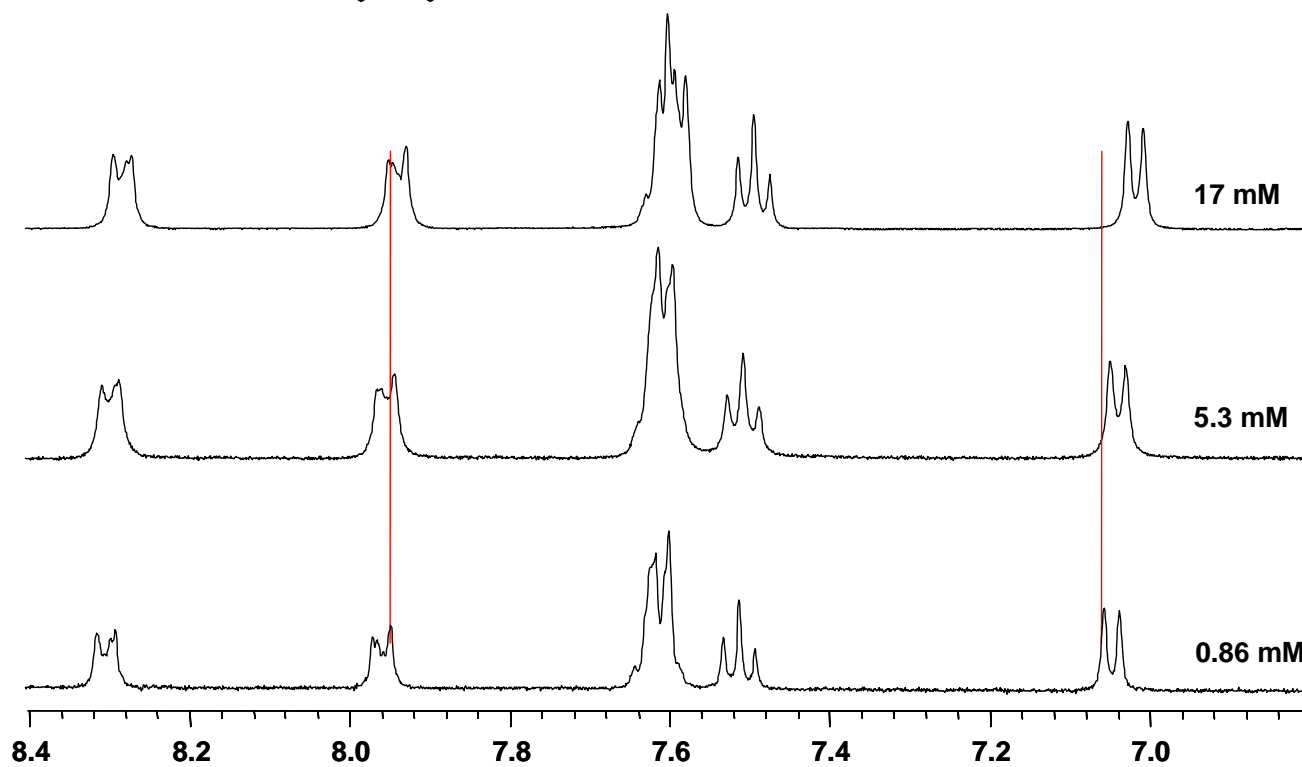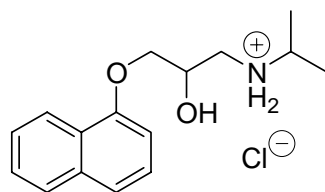
Figure S12 shows again some degree of complexation-induced shift, in addition to signal line broadening (volumes of propranolol stock solution added to the microgel stated next to each ^{1}H NMR spectrum). The shifts are indicative of binding. However, the effect is small since the aromatic protons are not near the binding site.

Effect of pH
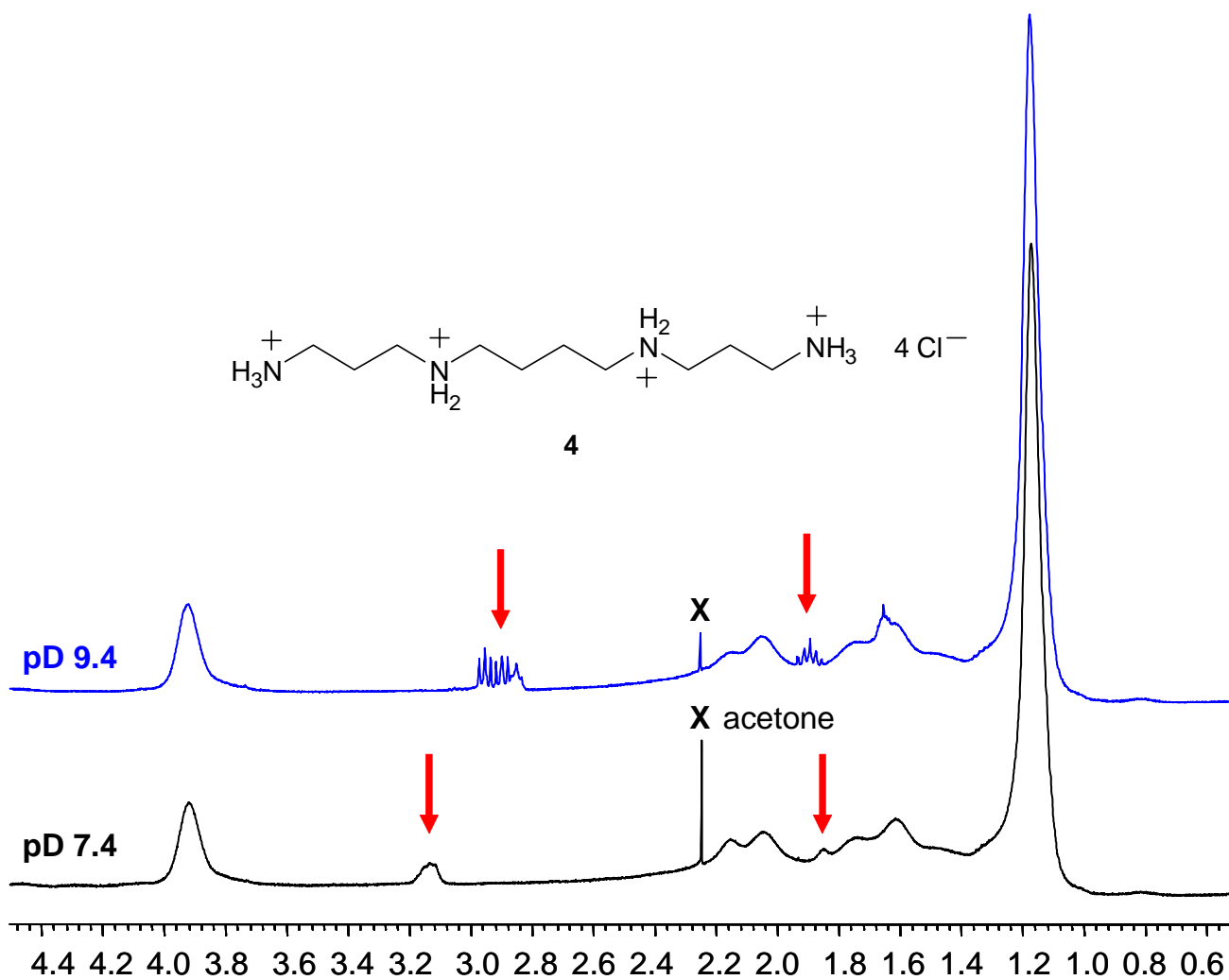
Figure S13. The two ^{1}H NMR spectra above show a combination of spermine and microgel in D_2O solution and were recorded at the same microgel–spermine concentrations but at different pD. Signals of the ligand are marked by arrows. The characteristic line broadening is not observed at pD 9.4 — indicating that the protonation of the amine groups is essential to binding.

^{1}H NMR titrations with a non-binding tetramethylammonium salt

Microgel + 2.7 mM NMe$_4$$^+$

Microgel + 8.0 mM NMe$_4$$^+$

2.7 mM NMe$_4$$^+$ in the absence of microgel

4.0   3.0   2.0

Microgel + 2.7 mM NMe$_4$$^+$

Microgel + 8.0 mM NMe$_4$$^+$

2.7 mM NMe$_4$$^+$ in the absence of microgel

3.28   3.26   3.24   3.22   3.20   3.18   3.16   3.14   3.12
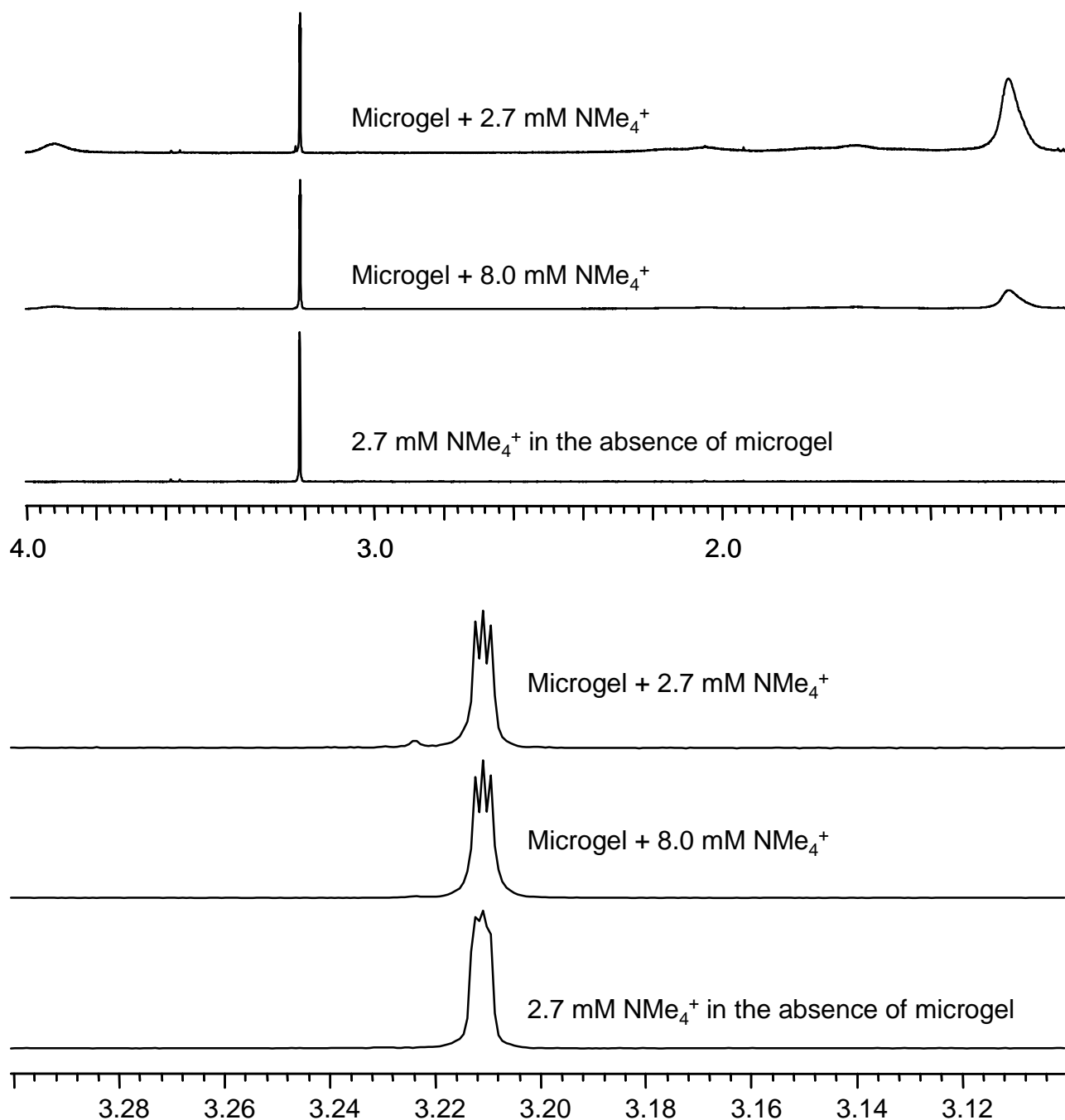
Figure S14. The above NMR spectra are the results of a ^{1}H NMR titration of microgel with tetramethylammonium hydroxide (NMe$_4$$^+$ OH$^-$) in pD 7.4 buffer solution. No changes in chemical shift or in line broadening were evident. The triplet structure (resulting from coupling of the methyl protons with ^{14}N) remains unaffected in the presence of microgel.
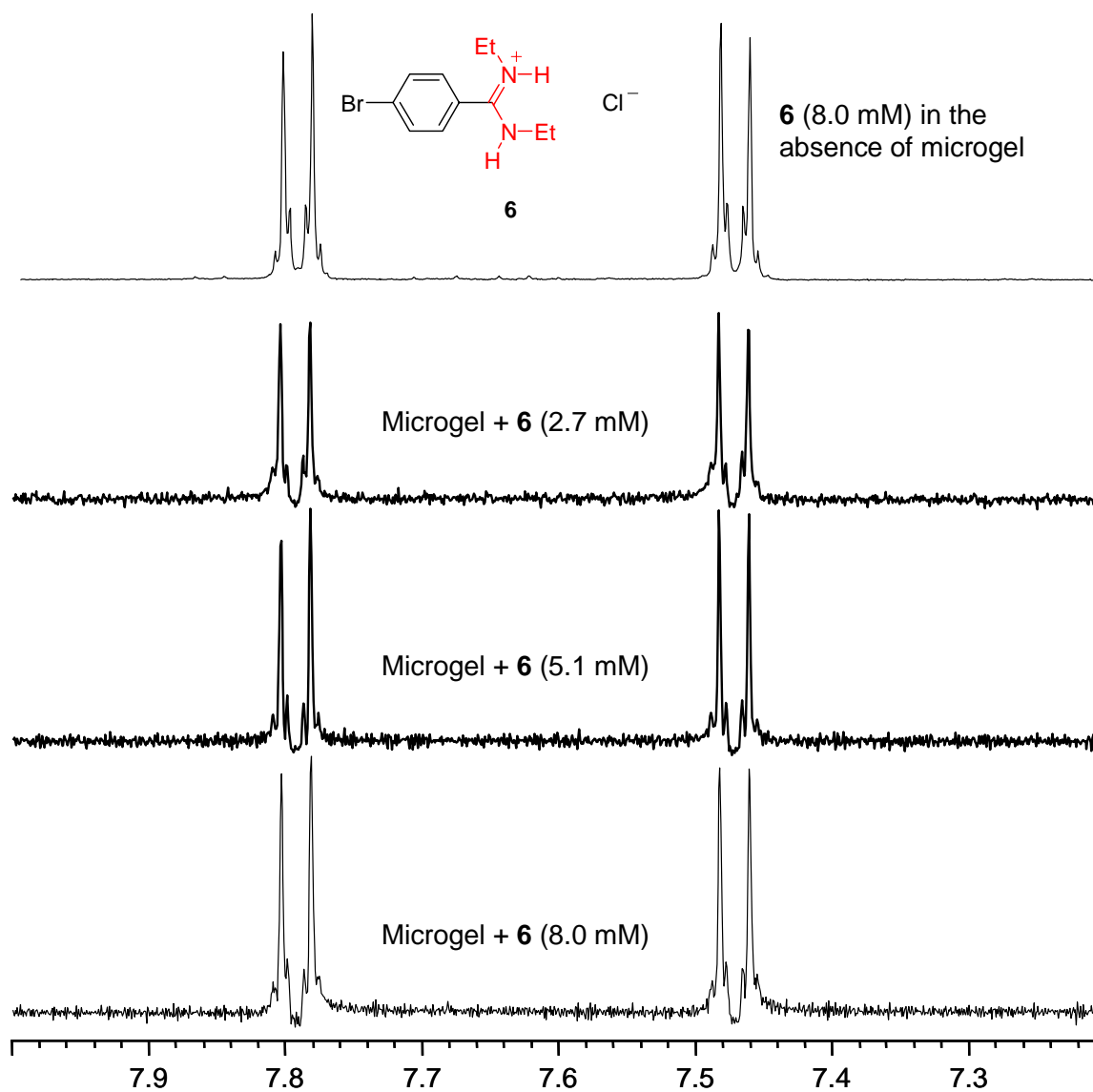
Figure S15. The aromatic signals of 4-bromo-*N,N*-diethylbenzamidinium chloride (**6**) show no complexation-induced signal shift in the presence of microgel. In addition, the fine structure of the AA'XX' multiplet remains, indicating that there is no line broadening as a result of binding.

Trilysine + microgel
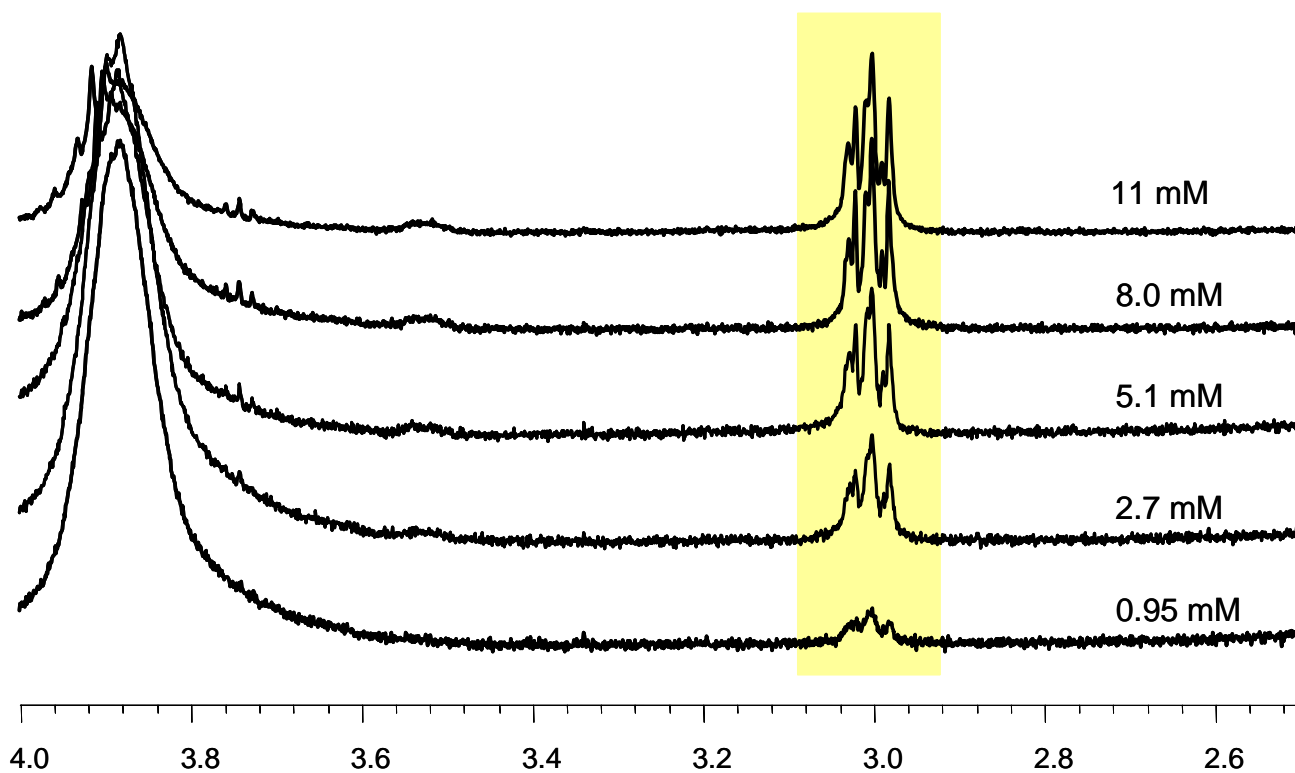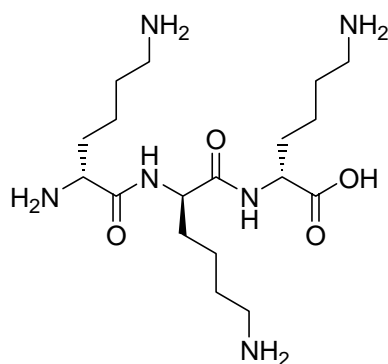
Figure S16 shows no complexation-induced changes in chemical shift and little signal line broadening indicative of binding of trilysine (H-Lys-Lys-Lys-OH, acetate salt) in the presence of microgel in D_2O (pH 7.4, ionic strength 0.15 M) at 25 °C. The absence of binding is most likely due to the flexibility of the tripeptide and the high ionic strength.

Trilysine + microgel — Effect of ionic strength
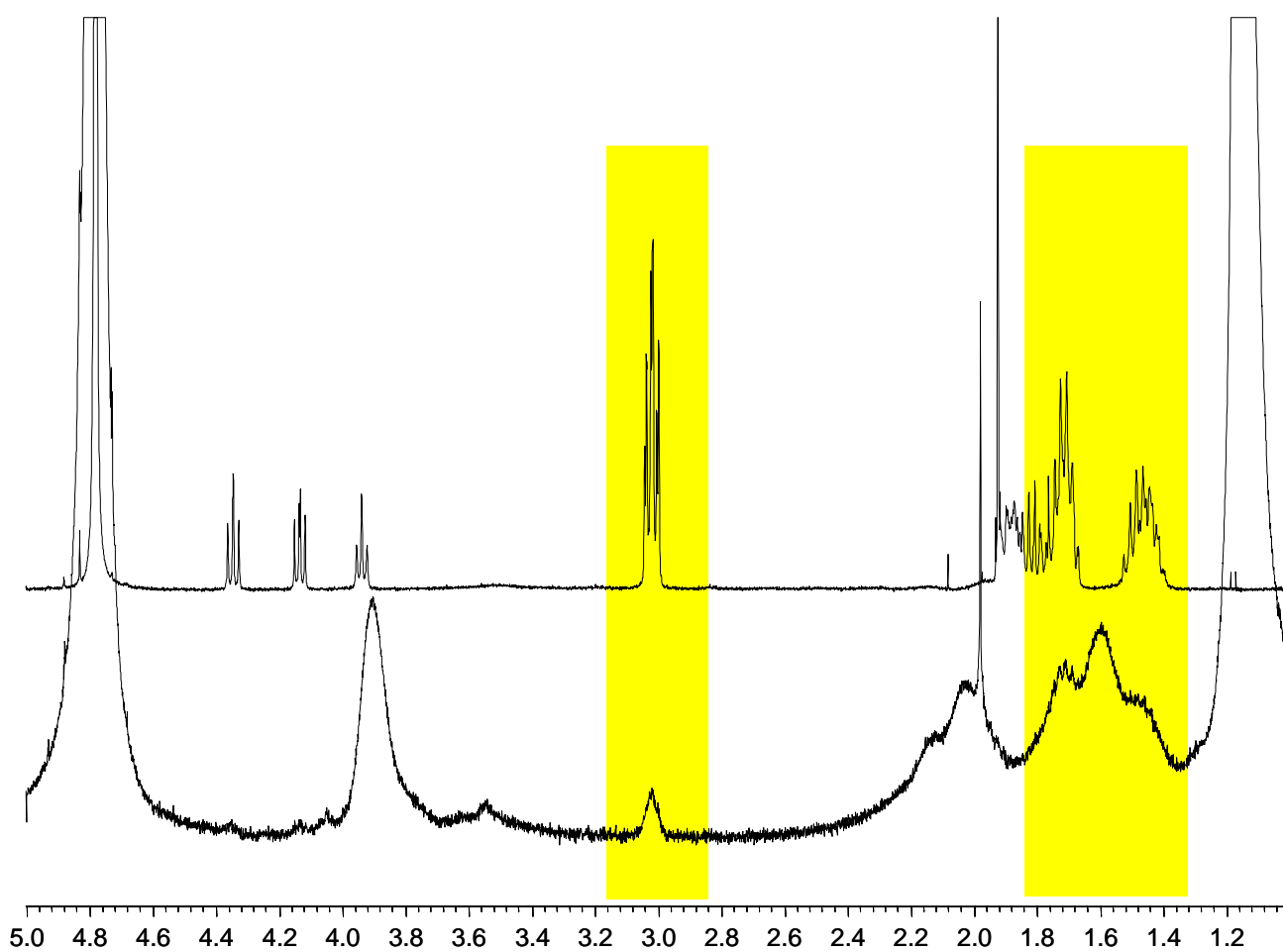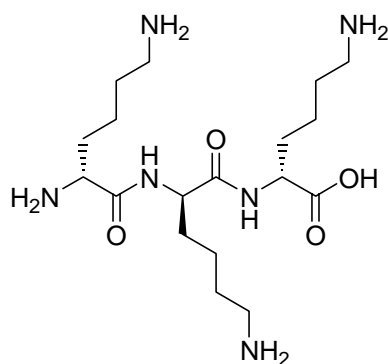
Figure S17. Top: ^{1}H NMR spectrum of trilysine (H-Lys-Lys-Lys-OH, acetate salt) in D_2O. Bottom: The tripeptide shows evidence of line-broadening in the presence of microgel in D_2O at 25 °C (bottom spectrum) when no electrolyte is added. This is an indication that binding occurs in this case but only as long as ionic strength of the aqueous solution is kept low.

NMR titration of spermine tetrahydrochloride with 3-Na in D₂O
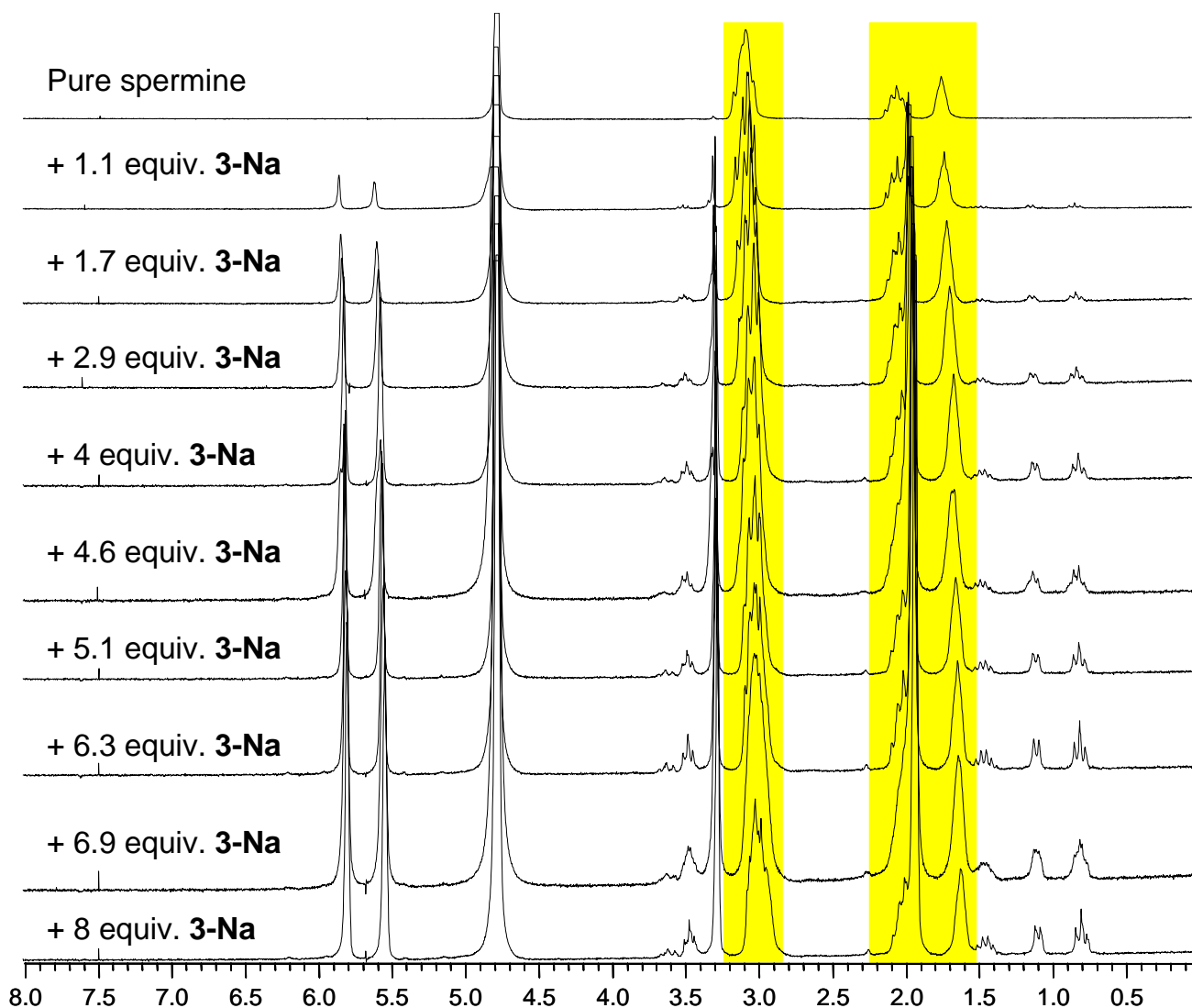
Figure S18. The ^{1}H NMR chemical shifts of the spermine CH_2 signals in D_2O show no change upon addition of monomer **3-Na**, indicating the absence of binding even at high concentration and large excess of the tetrazolate (spermine concentration: 0.05 M) and when no electrolyte was added. The highlighted signals refer to spermine. Data were obtained on a Bruker AC200 NMR spectrometer (200 MHz) at 25 °C.

Preparation of spermine model complex

Spermine **4** (360 mg, 1.78 mmol) and 5-methacrylamidotetrazole **3** (814 mg, 5.33 mmol) were dissolved in warm methanol (25 mL). Crystals were obtained by slow evaporation of methanol. Yield: 428 mg (39%). Anal. Calcd. for $C_{30}H_{54}N_{24}O_4$: C 44.2%, H 6.7%, N 41.3%. Found: C 44.3%, H 6.8%, N 41.0%.

X-ray crystallographic study of spermine model complex

Intensity data were collected on single crystals coated in Paratone-N oil and mounted with vacuum grease onto glass fibers, on an Oxford Diffraction Xcalibur-2 diffractometer with Mo Kα radiation at 120K, cooled by an Oxford Instruments Cryojet. Structures were solved by direct methods and refined by full matrix least squares refinement with F^2 data using the SHELXTL suite of programs. Hydrogen atoms were constrained to ideal geometries and their displacement parameters of all H atoms were treated at riding on the bound atom. The diffraction was very weak and no data were observed beyond 45 degrees in 2θ.

Table 1. Further crystal structure determination experimental details

_____

|	
Identification code	model complex
Empirical formula	C15 H27 N12 O2
Formula weight	407.49
Temperature	120(2) K
Wavelength	0.71073 Å
Crystal system	Monoclinic
Space group	$P2_1/c$
Unit cell dimensions	a = 11.1364(14) Å α= 90.000(12)°.
	b = 13.482(2) Å β= 110.275(12)°.
	c = 14.299(2) Å γ = 90.000(11)°.
Volume	2013.8(5) Å^3
Z	4
Density (calculated)	1.344 Mg/m^3
Absorption coefficient	0.097 mm^{-1}
F(000)	868
Crystal size	0.08 x 0.03 x 0.03 mm^3
Theta range for data collection	3.23 to 22.32°.
Index ranges	-9<=h<=9, -11<=k<=12, -13<=l<=14
Reflections collected	10445
Independent reflections	1959 [R(int) = 0.0707]
Completeness to theta = 22.32°	76.1 %
Absorption correction	None
Refinement method	Full-matrix least-squares on F^2
Data / restraints / parameters	1959 / 0 / 263
Goodness-of-fit on F2	1.257
Final R indices [I>2sigma(I)]	R1 = 0.1043, wR2 = 0.1277
R indices (all data)	R1 = 0.1479, wR2 = 0.1396
Extinction coefficient	0.0032(10)
Largest diff. peak and hole	0.175 and -0.161 e.Å-3
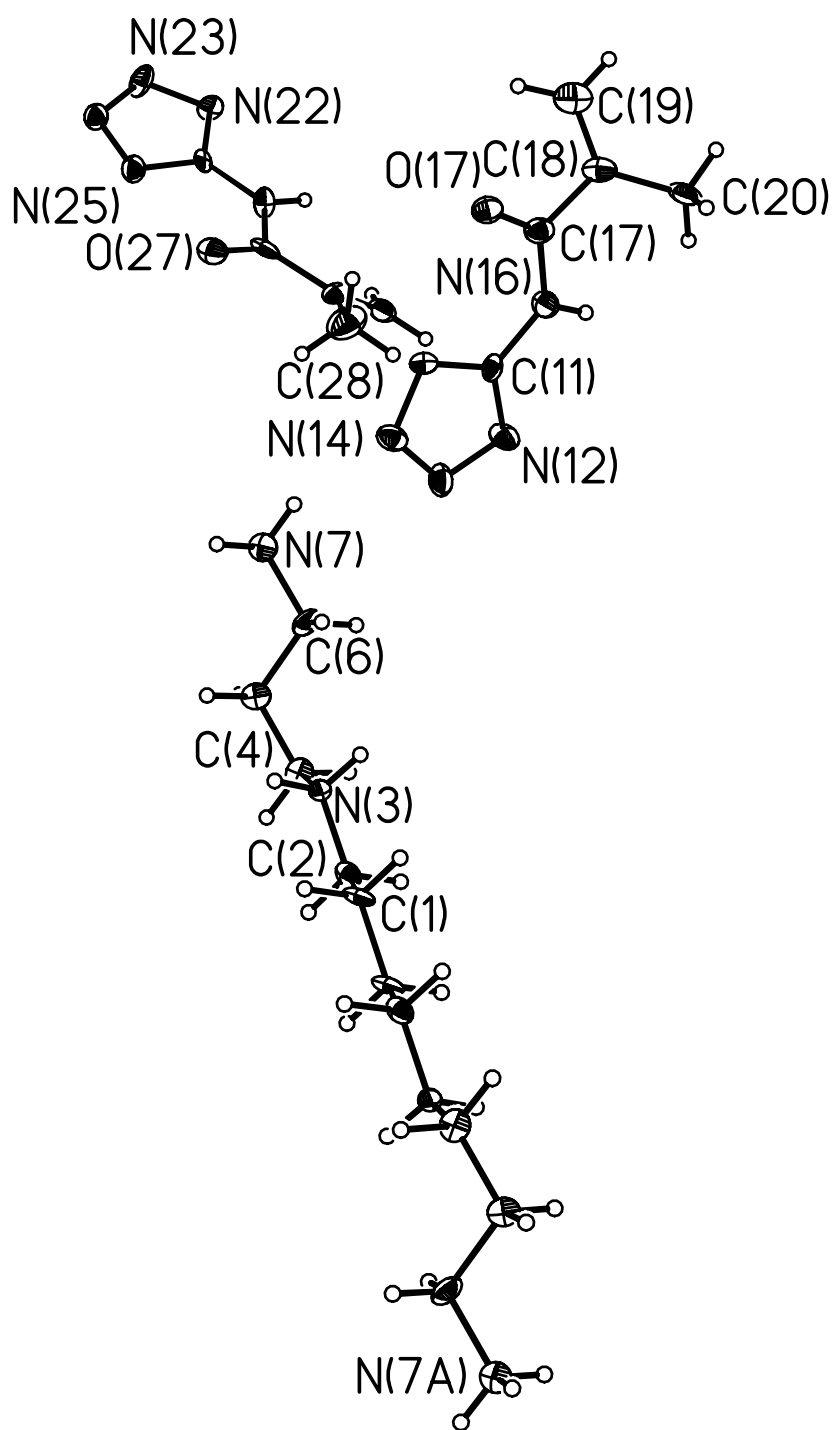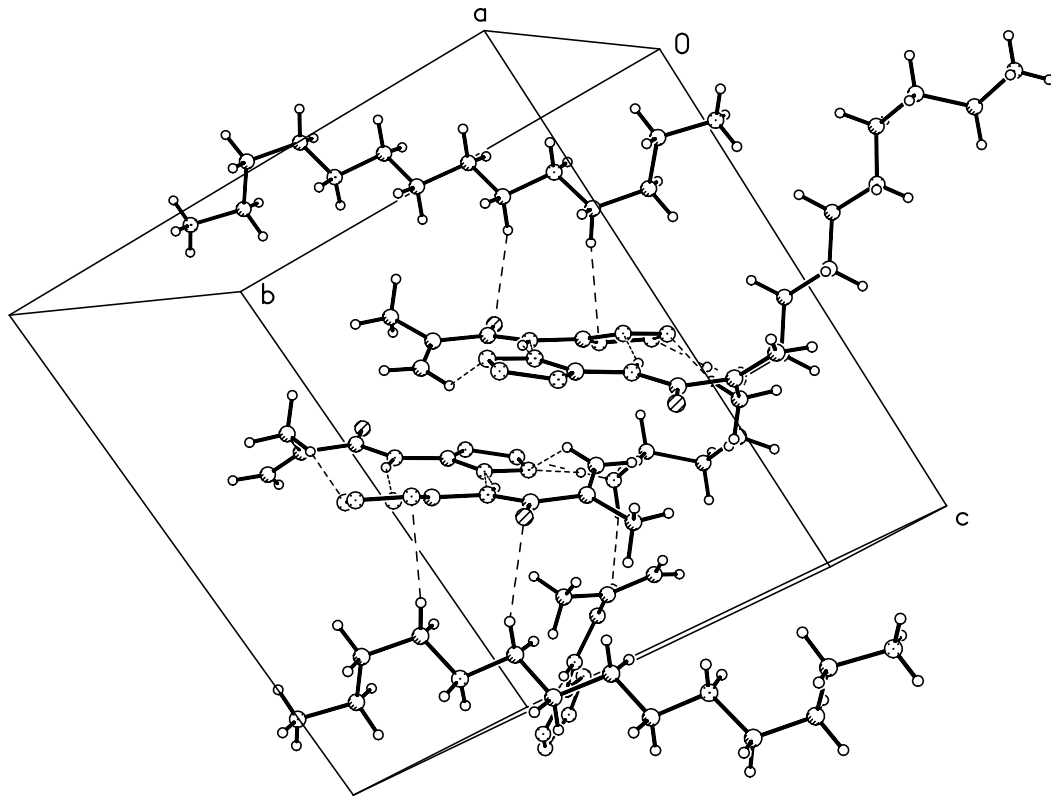
Table 2.   Bond lengths [Å] and angles [°] for model complex.
_____

C(1)-C(2)	1.505(9)	C(1)-C(1)#1	1.509(12)	C(1)-H(1A)	0.9900
C(1)-H(1B)	0.9900	C(2)-N(3)	1.480(7)	C(2)-H(2A)	0.9900
C(2)-H(2B)	0.9900	N(3)-C(4)	1.489(8)	N(3)-H(3A)	0.9200
N(3)-H(3B)	0.9200	C(4)-C(5)	1.505(9)	C(4)-H(4A)	0.9900
C(4)-H(4B)	0.9900	C(5)-C(6)	1.528(8)	C(5)-H(5A)	0.9900
C(5)-H(5B)	0.9900	C(6)-N(7)	1.505(8)	C(6)-H(6A)	0.9900
C(6)-H(6B)	0.9900	N(7)-H(7A)	0.9100	N(7)-H(7B)	0.9100
N(7)-H(7C)	0.9100	C(11)-N(15)	1.326(7)	C(11)-N(12)	1.328(8)
C(11)-N(16)	1.401(8)	N(12)-N(13)	1.351(7)	N(13)-N(14)	1.320(7)
N(14)-N(15)	1.368(7)	N(16)-C(17)	1.358(8)	N(16)-H(16)	0.8800
C(17)-O(17)	1.236(7)	C(17)-C(18)	1.503(9)	C(18)-C(19)	1.327(9)
C(18)-C(20)	1.493(8)	C(19)-H(19B)	0.9500	C(19)-H(19A)	0.9500
C(20)-H(20C)	0.9800	C(20)-H(20A)	0.9800	C(20)-H(20B)	0.9800
C(21)-N(25)	1.328(7)	C(21)-N(22)	1.329(8)	C(21)-N(26)	1.400(8)
N(22)-N(23)	1.363(7)	N(23)-N(24)	1.312(7)	N(24)-N(25)	1.354(7)
N(26)-C(27)	1.359(8)	N(26)-H(26)	0.8800	C(27)-O(27)	1.231(7)
C(27)-C(28)	1.497(9)	C(28)-C(29)	1.317(8)	C(28)-C(30)	1.499(9)
C(29)-H(29B)	0.9500	C(29)-H(29A)	0.9500	C(30)-H(30C)	0.9800
C(30)-H(30B)	0.9800	C(30)-H(30A)	0.9800		

C(2)-C(1)-C(1)#1	112.7(7)	C(2)-C(1)-H(1A)	109.0	C(1)#1-C(1)-H(1A)	109.0
C(2)-C(1)-H(1B)	109.0	C(1)#1-C(1)-H(1B)	109.0	H(1A)-C(1)-H(1B)	107.8
N(3)-C(2)-C(1)	111.6(5)	N(3)-C(2)-H(2A)	109.3	C(1)-C(2)-H(2A)	109.3
N(3)-C(2)-H(2B)	109.3	C(1)-C(2)-H(2B)	109.3	H(2A)-C(2)-H(2B)	108.0
C(2)-N(3)-C(4)	112.8(5)	C(2)-N(3)-H(3A)	109.0	C(4)-N(3)-H(3A)	109.0
C(2)-N(3)-H(3B)	109.0	C(4)-N(3)-H(3B)	109.0	H(3A)-N(3)-H(3B)	107.8
N(3)-C(4)-C(5)	113.4(5)	N(3)-C(4)-H(4A)	108.9	C(5)-C(4)-H(4A)	108.9
N(3)-C(4)-H(4B)	108.9	C(5)-C(4)-H(4B)	108.9	H(4A)-C(4)-H(4B)	107.7
C(4)-C(5)-C(6)	112.8(5)	C(4)-C(5)-H(5A)	109.0	C(6)-C(5)-H(5A)	109.0
C(4)-C(5)-H(5B)	109.0	C(6)-C(5)-H(5B)	109.0	H(5A)-C(5)-H(5B)	107.8
N(7)-C(6)-C(5)	111.5(5)	N(7)-C(6)-H(6A)	109.3	C(5)-C(6)-H(6A)	109.3
N(7)-C(6)-H(6B)	109.3	C(5)-C(6)-H(6B)	109.3	H(6A)-C(6)-H(6B)	108.0
C(6)-N(7)-H(7A)	109.5	C(6)-N(7)-H(7B)	109.5	H(7A)-N(7)-H(7B)	109.5
C(6)-N(7)-H(7C)	109.5	H(7A)-N(7)-H(7C)	109.5	H(7B)-N(7)-H(7C)	109.5
N(15)-C(11)-N(12)	114.3(6)	N(15)-C(11)-N(16)	124.9(7)	N(12)-C(11)-N(16)	120.7(6)
C(11)-N(12)-N(13)	103.9(5)	N(14)-N(13)-N(12)	109.2(5)	N(13)-N(14)-N(15)	109.9(5)

C(11)-N(15)-N(14)	102.7(5)	C(17)-N(16)-C(11)	125.6(6)	C(17)-N(16)-H(16)	117.2
C(11)-N(16)-H(16)	117.2	O(17)-C(17)-N(16)	123.9(6)	O(17)-C(17)-C(18)	120.4(7)
N(16)-C(17)-C(18)	115.6(6)	C(19)-C(18)-C(20)	123.4(6)	C(19)-C(18)-C(17)	117.7(6)
C(20)-C(18)-C(17)	118.8(6)	C(18)-C(19)-H(19B)	120.0	C(18)-C(19)-H(19A)	120.0
H(19B)-C(19)-H(19A)	120.0	C(18)-C(20)-H(20C)	109.5	C(18)-C(20)-H(20A)	109.5
H(20C)-C(20)-H(20A)	109.5	C(18)-C(20)-H(20B)	109.5	H(20C)-C(20)-H(20B)	109.5
H(20A)-C(20)-H(20B)	109.5	N(25)-C(21)-N(22)	114.2(6)	N(25)-C(21)-N(26)	125.1(7)
N(22)-C(21)-N(26)	120.7(6)	C(21)-N(22)-N(23)	103.4(5)	N(24)-N(23)-N(22)	109.0(5)
N(23)-N(24)-N(25)	110.6(5)	C(21)-N(25)-N(24)	102.8(5)	C(27)-N(26)-C(21)	124.1(6)
C(27)-N(26)-H(26)	118.0	C(21)-N(26)-H(26)	118.0	O(27)-C(27)-N(26)	122.5(6)
O(27)-C(27)-C(28)	120.2(7)	N(26)-C(27)-C(28)	117.2(6)	C(29)-C(28)-C(27)	123.2(7)
C(29)-C(28)-C(30)	122.0(6)	C(27)-C(28)-C(30)	114.8(6)	C(28)-C(29)-H(29B)	120.0
C(28)-C(29)-H(29A)	120.0	H(29B)-C(29)-H(29A)	120.0	C(28)-C(30)-H(30C)	109.5
C(28)-C(30)-H(30B)	109.5	H(30C)-C(30)-H(30B)	109.5	C(28)-C(30)-H(30A)	109.5
H(30C)-C(30)-H(30A)	109.5	H(30B)-C(30)-H(30A)	109.5		

Symmetry transformations used to generate equivalent atoms: #1 -x+2,-y+2,-z+1

Table 3. Torsion angles [°] for model complex.

C(1)#1-C(1)-C(2)-N(3)	179.2(6)	C(1)-C(2)-N(3)-C(4)	-172.5(5)
C(2)-N(3)-C(4)-C(5)	168.1(5)	N(3)-C(4)-C(5)-C(6)	66.4(7)
C(4)-C(5)-C(6)-N(7)	176.6(5)	N(15)-C(11)-N(12)-N(13)	-1.0(8)
N(16)-C(11)-N(12)-N(13)	-177.1(6)	C(11)-N(12)-N(13)-N(14)	0.6(7)
N(12)-N(13)-N(14)-N(15)	0.0(7)	N(12)-C(11)-N(15)-N(14)	1.0(8)
N(16)-C(11)-N(15)-N(14)	176.8(6)	N(13)-N(14)-N(15)-C(11)	-0.6(7)
N(15)-C(11)-N(16)-C(17)	5.7(10)	N(12)-C(11)-N(16)-C(17)	-178.7(7)
C(11)-N(16)-C(17)-O(17)	3.9(10)	C(11)-N(16)-C(17)-C(18)	-173.9(6)
O(17)-C(17)-C(18)-C(19)	-43.9(10)	N(16)-C(17)-C(18)-C(19)	133.9(7)
O(17)-C(17)-C(18)-C(20)	135.9(7)	N(16)-C(17)-C(18)-C(20)	-46.2(9)
N(25)-C(21)-N(22)-N(23)	-0.2(7)	N(26)-C(21)-N(22)-N(23)	179.9(5)
C(21)-N(22)-N(23)-N(24)	0.5(6)	N(22)-N(23)-N(24)-N(25)	-0.6(7)
N(22)-C(21)-N(25)-N(24)	-0.2(7)	N(26)-C(21)-N(25)-N(24)	179.8(6)
N(23)-N(24)-N(25)-C(21)	0.5(7)	N(25)-C(21)-N(26)-C(27)	-13.9(10)

N(22)-C(21)-N(26)-C(27)	166.1(6)	C(21)-N(26)-C(27)-O(27)		-6.3(10)
C(21)-N(26)-C(27)-C(28)	176.5(6)	O(27)-C(27)-C(28)-C(29)		159.2(6)
N(26)-C(27)-C(28)-C(29)	-23.6(9)	O(27)-C(27)-C(28)-C(30)		-17.7(9)
N(26)-C(27)-C(28)-C(30)	159.6(6)			

Symmetry transformations used to generate equivalent atoms: #1 -x+2,-y+2,-z+1

Table 4. Hydrogen bonds for model complex [Å and °].

D-H...A	d(D-H)	d(H...A)	d(D...A)	<(DHA)
N(3)-H(3A)...N(24)#2	0.92	1.90	2.802(8)	165
N(3)-H(3A)...N(23)#2	0.92	2.63	3.365(7)	137
N(3)-H(3B)...N(15)#3	0.92	1.92	2.749(8)	150
N(3)-H(3B)...O(17)#3	0.92	2.43	3.115(6)	131
N(7)-H(7A)...O(17)#4	0.91	2.08	2.966(7)	165
N(7)-H(7B)...N(14)	0.91	1.98	2.852(7)	159
N(7)-H(7B)...N(13)	0.91	2.59	3.245(7)	130
N(7)-H(7C)...O(27)#5	0.91	2.17	2.975(6)	148
N(7)-H(7C)...N(25)#5	0.91	2.20	2.914(7)	134
N(16)-H(16)...N(22)#6	0.88	2.18	3.027(7)	160
N(26)-H(26)...N(12)#7	0.88	2.09	2.933(7)	161

Symmetry transformations used to generate equivalent atoms:

#1 -x+2,-y+2,-z+1   #2 x,-y+1/2,z+1/2   #3 -x+2,-y+1,-z+1

#4 x,-y+1/2,z-1/2   #5 -x+2,y+1/2,-z+1/2   #6 -x+1,y+1/2,-z+1/2

#7 -x+1,y-1/2,-z+1/2